# Coupling finite and boundary element methods using a localized adaptive radiation condition for the Helmholtz's equation

Y. Boubendir[1], A. Bendali[2], and N. Zerbib[3]

## 1 Introduction

In this paper, we are interested in impenetrable surfaces with relatively large size on which a heterogeneous object of relatively small size is posed. In this case, a straightforward FEM-BEM (finite and boundary element methods) coupling leads to a linear system of very large scale difficult to solve [7]. In this work, we propose an alternative method derived from a modification of the adaptive radiation condition approach ([11, 1, 12]). This technique consists of enclosing the computational domain by an artificial truncating surface on which the adaptive radiation condition is posed. This condition is expressed using integral operators acting as a correction term of the absorbing boundary condition. However, enclosing completely the computational domain by an artificial surface in this range leads to problems with very large size, and results in very slow convergence of the iterative procedure. We propose to localize this surface only around the heterogenous region, which will generates a relatively small bounded domain dealt with by a FEM, and suitably coupled with a BEM expressing the solution on the impenetrable surface. The resulting formulation, based on a particular overlapping domain decomposition method, is solved iteratively where FEM and BEM linear systems are solved separately. The wave problem considered in this paper is stated as follows

$$\begin{cases} \nabla \cdot (\chi \nabla u) + \chi \kappa^2 n^2 u = 0 \quad \text{in } \Omega, \\ \chi \partial_{\mathbf{n}} u = -f \text{ on } \Gamma, \\ \lim_{|x|\to\infty} |x|^{1/2} (\partial_{|x|} u - i\kappa u) = 0, \end{cases} \tag{1}$$

Department of Mathematical Sciences and Center for Applied Mathematics and Statistics, NJIT, Univ. Heights. 323 Dr. M. L. King Jr. Blvd, Newark, NJ 07102, USA. boubendi@njit.edu · University of Toulouse, INSA de Toulouse, Institut Mathématique de Toulouse, UMR CNRS 5219, 135 avenue de Rangueil F31077, Toulouse cedex 1, France. abendali@insa-toulouse.fr · ESI Group, 20 rue du Fonds Pernant, 60471 Compiegne Cedex, France. nicolas.zerbib@esi-group.com

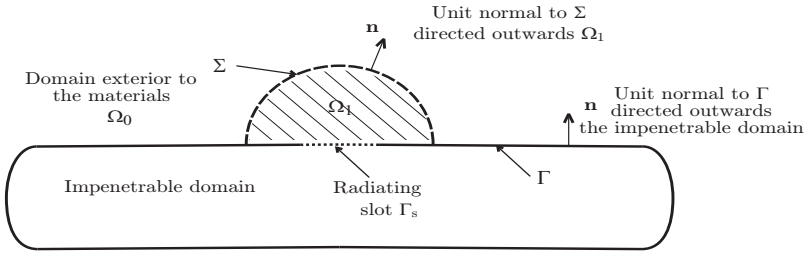


**Fig. 1** Non-overlapping decomposition of the exterior domain $\Omega$ into $\Omega_0$ and $\Omega_1$.

where $\Omega$ is the complement of the impenetrable obstacle. We indicate by $\Omega_1$ a bounded domain filled by a possibly heterogeneous material and posed on a slot $\Gamma_{\text{slot}}$ on which are applied the sources producing the radiated wave $u$. The interface $\Sigma$ separates $\Omega_1$ from the free propagation domain $\Omega_0$, $\mathbf{n}$ denotes the normal to $\Gamma$ or to $\Sigma$ directed outwards respectively the impenetrable obstacle enclosed by $\Gamma$ or the domain $\Omega_1$ (see Figure 1 ), $\chi$ and $n$ indicate, respectively, the relative dielectric permittivity and the relative magnetic permeability, and $\kappa$ is the wave number. Let us note finally that $\chi = n = 1$ in $\Omega_0$. For the sake of presentation, we express problem (1) in the form of the following system

$$\begin{cases} \Delta u_0 + \kappa^2 u_0 = 0 \text{ in } \Omega_0, \\ \partial_{\mathbf{n}} u_0 = 0 \text{ on } \Gamma \cap \partial\Omega_0, \\ \lim_{|x|\to\infty} |x|^{1/2}(\partial_{|x|} u_0 - i\kappa u_0) = 0, \end{cases} \tag{2}$$

$$\begin{cases} \nabla \cdot (\chi \nabla u_1) + \chi \kappa^2 n^2 u_1 = 0 \text{ in } \Omega_1, \\ \chi \partial_{\mathbf{n}} u_1 = -f \text{ on } \Gamma \cap \partial\Omega_1. \end{cases} \tag{3}$$

These boundary-value problems are coupled on $\Sigma$ through the transmission conditions

$$u_0 = u_1, \quad \partial_{\mathbf{n}} u_0 = \chi \partial_{\mathbf{n}} u_1. \tag{4}$$

## 2 The adaptive localized radiation condition

To localize the truncating interface only around the penetrable material, Fig. 2, we introduce a fictitious boundary $S$ which in turn produces the bounded domain $\Omega_S$ limited by $S$ and the impenetrable zone. The goal is to derive a formulation of problem (1) as a coupled system composed of two equations with two unknowns $u_0$ and $u_S$ where the function $u_S = u|_{\Omega_S}$ is approximated by a FEM, and $u_0$, already defined above, is computed using an integral equation on $\Gamma_\Sigma$ (Figure 3). The integral representation of the function $u_0$ is given in terms of a single- and a double-layer potential created by densities on $\Gamma_\Sigma$, and as a result can be seen as the restriction to $\Omega_0$ of

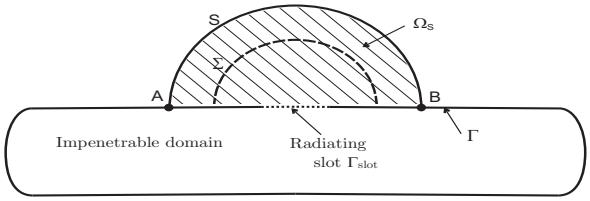


**Fig. 2** The bounded domain $\Omega_S$ and the fictitious boundary $S$ on which is posed the adaptive radiation condition.

the solution of a transmission problem posed on all of the plane $\mathbb{R}^2$ (cf., e.g., [10, 14, 13]). In view of the equations that are set in $\Omega_S$, we are in the case of a particular decomposition with an overlap of the computational domain (see similar ideas in [4, 3] for the usual adaptive radiation condition). However, it will be more convenient not to distinguish $u_0$ from $u_S$ and to refer to them as the same function $u$ in $H^1_{\text{loc}}(\overline{\Omega})$. Simply by restricting $u$ to $\Omega_S$, we get from (1) that $u$ satisfies

$$\begin{cases} \nabla \cdot (\chi \nabla u) + \chi \kappa^2 n^2 u = 0, & \text{in } \Omega_S, \\ \chi \partial_{\mathbf{n}} u = -f & \text{on } \Gamma \cap \partial\Omega_S. \end{cases} \tag{5}$$

In $\Omega_0$, we use the integral representations of the solutions to the Helmholtz equation satisfying the Sommerfeld radiation condition (cf., e.g., [14, 8, 9, 6])

$$u(x) = V^{*,\Sigma} p(x) - N^{*,\Gamma_\Sigma} u(x), \quad x \in \Omega_0, \tag{6}$$

with

$$V^{*,\Sigma} p(x) = \int_\Sigma G(x,y) p(y)\ ds_y \tag{7}$$

$$p = -\chi \partial_{\mathbf{n}} u|_\Sigma \tag{8}$$

$$N^{*,\Gamma_\Sigma} u(x) = -\int_{\Gamma_\Sigma} \partial_{n_y} G(x,y) u(y)\ ds_y \tag{9}$$

where $G(x,y) = (i/4) H_0^{(1)}(\kappa|x-y|)$ for $x \neq y \in \mathbb{R}^2$.

The derivation of the FEM-BEM coupling procedure can be introduced starting from the following Green formula

$$\int_{\Omega_S} \chi \left( \nabla u \cdot \nabla v - \kappa^2 n^2 uv \right) dx = \langle \partial_{\mathbf{n}} u, v \rangle_{\widetilde{H}^{-1/2}(S), H^{1/2}(S)} + \langle f, v \rangle_{\widetilde{H}^{-1/2}(\Gamma_{\text{slot}}), H^{1/2}(\Gamma_{\text{slot}})} \tag{10}$$

where $\langle \cdot, \cdot \rangle_{\widetilde{H}^{-1/2}(S), H^{1/2}(S)}$ denotes the duality pairing between $\widetilde{H}^{-1/2}(S)$ and $H^{1/2}(S)$, and $v$ is an arbitrary test function in $H^1_{\text{loc}}(\overline{\Omega})$. The space $\widetilde{H}^{-1/2}(S)$

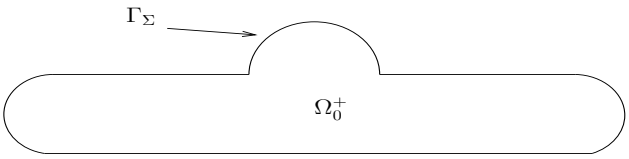


**Fig. 3** Representation of $\Omega_0^+$ and its boundary $\Gamma_\Sigma$.

is defined similarly to $\widetilde{H}^{-1/2}(\Gamma_{\rm slot})$ (cf. [5, 13] for the definition of Sobolev spaces).

The localized adaptive radiation condition approach (LRC) uses an iterative method to solve problem (10) where the term $\partial_{\mathbf{n}} u$, at the right-hand side, is updated at each iteration. However, there is no garantee that problem (10) can be safely solved. To avoid these kinds of difficulties, we introduce the stabilization term $-i\kappa \int_S uv \; ds$ in both sides of (10). On the other hand, $S$ is an open curve having its end-points $A$ and $B$ on $\Gamma$ (see Fig. 2). To prevent singular integrals near these points, we introduce a cut-off function $\eta \in \mathcal{D}(\mathbb{R}^2)$ such that $0 \leq \eta \leq 1$, $\eta = 1$ on $S$, except small neighborhood of any of $A$ and $B$, $\eta$ being moreover equal to 0 around $A$ and $B$, and write (10) in the following form

$$\begin{aligned}\int_{\Omega_S} \chi \left(\nabla u \cdot \nabla v - \kappa^2 n^2 uv\right) dx - i\kappa \int_S \eta uv \; ds = \langle \partial_{\mathbf{n}} u, v \rangle_{\widetilde{H}^{-1/2}(S), H^{1/2}(S)} \\ -i\kappa \int_S \eta uv \; ds + \langle f, v \rangle_{\widetilde{H}^{-1/2}(\Gamma_{\rm slot}), H^{1/2}(\Gamma_{\rm slot})} \,.\end{aligned} \tag{11}$$

Consider now the curve $\Gamma_S$ obtained by joining $S$ and the part of $\Gamma$ outside $\Omega_S$ and express that $\partial_{\mathbf{n}} u = 0$ there outside $S$ variationally as follows

$$\langle \partial_{\mathbf{n}} u, v \rangle_{\widetilde{H}^{-1/2}(S), H^{1/2}(S)} = \langle \partial_{\mathbf{n}} u, v \rangle_{H^{-1/2}(\Gamma_S), H^{1/2}(\Gamma_S)} \,, \tag{12}$$

for all test function $v$. We then get

$$\begin{aligned}\int_{\Omega_S} \chi \left(\nabla u \cdot \nabla v - \kappa^2 n^2 uv\right) dx - i\kappa \int_S \eta uv \; ds = \\ \langle \partial_{\mathbf{n}} u, v \rangle_{H^{-1/2}(\Gamma_S), H^{1/2}(\Gamma_S)} - i\kappa \int_S \eta uv \; ds + \langle f, v \rangle_{\widetilde{H}^{-1/2}(\Gamma_{\rm slot}), H^{1/2}(\Gamma_{\rm slot})}\end{aligned} \tag{13}$$

where the traces in the right-hand side are expressed from the integral representation (6) of $u$

$$\begin{cases} \eta u|_S = \eta V^{S,\Sigma} p - \eta N^{S,\Gamma_\Sigma} u \\ \partial_{\mathbf{n}} u|_{\Gamma_S} = \partial_{\mathbf{n}} V^{\Gamma_S,\Sigma} p - \partial_{\mathbf{n}} N^{\Gamma_S,\Gamma_\Sigma} u. \end{cases} \tag{14}$$

Clearly, since $\Sigma$ and $S$ share no common point and $\eta$ is zero in the proximity of the end-points of $S$, if $p$ and $u$ are sufficiently smooth functions, say for

example continuous, only the integral corresponding to $\partial_{\mathbf{n}} N^{*,\Gamma_\Sigma} u$ in (14) is an improper integral which can be expressed by means of a weakly singular kernel as follows

$$\begin{aligned}\left\langle \partial_{\mathbf{n}} N^{\Gamma_S,\Gamma_\Sigma} u, v\right\rangle_{H^{-1/2}(\Gamma_S),H^{1/2}(\Gamma_S)} &= \left\langle \partial_s v, V^{\Gamma_S,\Gamma_\Sigma} \partial_s u\right\rangle_{H^{-1/2}(\Gamma_S),H^{1/2}(\Gamma_S)} \\ &\quad -\kappa^2 \left\langle v\boldsymbol{\tau}, V^{\Gamma_S,\Gamma_\Sigma}\left(u\boldsymbol{\tau}\right)\right\rangle_{H^{-1/2}(\Gamma_S),H^{1/2}(\Gamma_S)}\end{aligned} \tag{15}$$

from a slight adaptation of the case where $\Gamma_S = \Gamma_\Sigma$ (cf., e.g., [10, p. 5]). The superscripts in the integral operators indicate that they correspond to a potential created by a density on $\Gamma_\Sigma$ and evaluated on $\Gamma_S$, and $\boldsymbol{\tau}$ is the unit tangent vector pointing in the growth direction of the arc length $s$.

In order to be able to use a nodal approximation of (13), we use a standard technique for gluing finite element approximations of different kinds or associated with non-conforming meshes generally called mortar FEM (cf., e.g., [2]). It is worth mentioning that here only standard meshes and finite element methods of the same kind are used. This way to proceed is just considered as a tool providing an approximation for the additional unknown $p$ in the framework of a nodal finite elemnt method. This technique consists in breaking the continuity across $\Sigma$ that $u$ is compelled to satisfy a priori and to express it as a constraint. The Lagrange multiplier corresponding to this constraint will be precisely the unknown $p$. It is hence more convenient to denote by separate symbols: $u_0$ for the restriction of $u$ to $\Omega_0 \cap \Omega_S$ and $\Gamma_\Sigma$ and $u_1$ for its restriction to $\Omega_1$. More precisely, we will use the following functional framework

$$\begin{cases} X_0 = \{u_0 \text{ defined (a.e.) on } \Omega_0 \cap \Omega_S \text{ and } \Gamma_\Sigma; \\ \qquad\qquad \exists U \in H^1(\Omega_0), U|_{\Gamma_\Sigma} = u_0|_{\Gamma_\Sigma} \text{ and } U|_{\Omega_0\cap\Omega_S} = u_0|_{\Omega_0\cap\Omega_S}\} \\ X_1 = H^1(\Omega_1), \quad X = X_0 \times X_1, \end{cases} \tag{16}$$

relation (8) and (13) to write

$$\begin{aligned}&\int_{\Omega_S\cap\Omega_0} \left(\nabla u_0 \cdot \nabla v_0 - \kappa^2 u_0 v_0\right) dx - i\kappa \int_S \eta u_0 v \; ds \\ &\quad + \int_{\Omega_1} \chi \left(\nabla u_1 \cdot \nabla v_1 - \kappa^2 n^2 u_1 v_1\right) dx + \langle p, v_1 - v_0\rangle_{\widetilde{H}^{-1/2}(\Sigma),H^{1/2}(\Sigma)} = \\ &\qquad \langle \partial_{\mathbf{n}} u, v_0\rangle_{H^{-1/2}(\Gamma_S),H^{1/2}(\Gamma_S)} - i\kappa \int_S \eta u v_0 \; ds + \langle f, v_1\rangle_{\widetilde{H}^{-1/2}(\Gamma_{\text{slot}}),H^{1/2}(\Gamma_{\text{slot}})}\end{aligned}$$

for all $(v_0, v_1) \in X$. Using then the integral represensation of $\partial_{\mathbf{n}} u|_{\Gamma_S}$ and $u|_S$ given above in (14), we readily arrive to the formulation effectively used to solve problem (1) numerically

$$\begin{cases} (u,p) \in X \times M, \; \forall\, (v,q) \in X \times M \\ a(u,v) + d(u_0,v_0) + b(p,v) + r(p,v_0) = \langle f, v_1\rangle_{\widetilde{H}^{-1/2}(\Gamma_{\text{slot}}),H^{1/2}(\Gamma_{\text{slot}})} \\ b(q,u) = 0 \end{cases} \tag{17}$$

with the following notation

$$\begin{cases} a_0(u_0, v_0) = \displaystyle\int_{\Omega_S \cap \Omega_0} \left(\nabla u_0 \cdot \nabla v_0 - \kappa^2 u_0 v_0\right) dx - i\kappa \int_S \eta u_0 v_0 ds, \\ a_1(u_1, v_1) = \displaystyle\int_{\Omega_1} \chi \left(\nabla u_1 \cdot \nabla v_1 - \kappa^2 n^2 u_1 v_1\right) dx, \\ a(u, v) = a_0(u_0, v_0) + a_1(u_1, v_1), \\ d(u_0, v_0) = \left\langle \partial_{\mathbf{n}} N^{\Gamma_S, \Gamma_\Sigma} u_0, v_0 \right\rangle_{H^{-1/2}(\Gamma_S), H^{1/2}(\Gamma_S)} - i\kappa \displaystyle\int_S \eta v_0 N^{S,\Sigma} u_0 ds \\ r(p, v_0) = -\displaystyle\int_{\Gamma_S} v_0 \partial_{\mathbf{n}} V^{\Gamma_S, \Sigma} p \; ds + i\kappa \int_S \eta v_0 V^{S,\Sigma} p \; ds, \\ b(p, v) = \left\langle p, v_1 - v_0 \right\rangle_{\widetilde{H}^{-1/2}(\Sigma), H^{1/2}(\Sigma)}, \end{cases} \tag{18}$$

and $M = \widetilde{H}^{-1/2}(\Sigma)$. We refer to [5] for the analysis of the well-posedness and the stability of (17).

## 3 Numerical results

To validate the LRC method, we will compare it with a direct FEM-BEM coupling and a domain decomposition one noted P-DDM (see [5] for more details about this method). The reference solution will be given by BE formulation (boundary elements) known to be the less dispersive. The geometry considered here (Fig. 4) depends on a parameter $L$ used to set a large size for the impenetrable domain relatively to the zone meshed in triangles as shown in Fig. 4. By varying this parameter, we test each numerical technique in terms of accuracy, CPU time, and convergence for the iterative ones. The lengths are expressed in wavelength units. To be able to compare the LRC formulation with the BE one, we suppose $\chi$ and $n$ constant in $\Omega_1$. More precisely, we choose $\chi = 1/4$ and $n = 2(1 + i)$, which correspond to a magnetic material in electromagnetism. The sources are located on the segment $\{x_2 = 0,\ -0.25 < x_1 < 0.25\}$ and are given by the Gaussian function $f(x_1) = -\exp(-(10x_1)^2)$.

The mesh used is of 20 points by wavelength in the free propagation zone and 15 points by wavelength in the material for the FEM-BEM formulations. The BE formulation is meshed using 20 points by wavelength for both the free propagation zone and the material. All the iterative methods are solved using the GMRES algorithm (cf., e.g. [15]). The first test concerns the case of a moderately elongated impenetrable domain corresponding to $L = 4$ and the second, much more elongated, is obtained for $L = 50$. Table 1 summarizes the numerical for each method in terms of accuracy and CPU time. For the iterative methods, we also compute the iteration number, noted "Iter" in

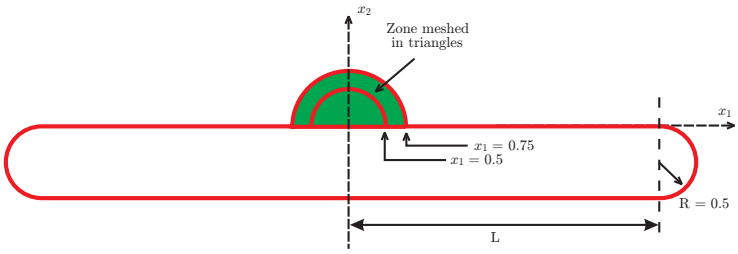


**Fig. 4** Geometry of the test-case

| | L | CPU | $\mathcal{E}$ | Iter |
|---|---|---|---|---|
| **BE** | 4 | 3 | – | – |
| | 50 | 94 | – | – |
| **FEBE** | 4 | 19 | 0.14 | – |
| | 50 | 169 | 0.14 | – |
| **LRC** | 4 | 38 | 0.17 | 11 |
| | 50 | 148 | 0.23 | 11 |
| **P-DDM** | 4 | 13 | 0.14 | 30 |
| | 50 | 127 | 0.14 | 30 |

**Table 1** Comparison of the various formulations in terms of accuracy, CPU time, and number of iterations.

Table 1, obtained by reducing the residual by a factor $10^{-6}$. To measure the accuracy, we use the quantity $\mathcal{E} = \max |s(\theta) - s_{\mathrm{BE}}(\theta)|$ where $s_{\mathrm{BE}}(\theta)$ is the far field computed by the BE approach.

The results reported in Table 1 confirm the robustness of the LRC formulation, it keeps the accuracy of the FEBE and P-DDM approaches. The CPU time used by the different methods also clearly shows the advantage of decoupling the solution of the sparse and the dense parts in the problem. Even if usual DDMs exhibit the same efficiency in terms of number of iterations and accuracy, their related iterative procedures may break down if the corresponding boundary-value problems set in the interior domain $\Omega_1$ present a resonance at the considered frequency, contrary to the LRC approach, see [5] for more explanations and numerical results. Another remarkable feature is that all the iterative procedures require the same number of iterations to converge for small to very large impenetrable domains.

## Acknowledgments

Y. Boubendir gratefully acknowledges support from NSF through grant No. DMS-1319720.

## References


[1] S. Alfonzetti, G. Borzì, and N. Salerno. Iteratively-improved Robin boundary conditions for the finite element solution of scattering problems in unbounded domains. *Int. J. Numer. Meth. Engng*, 42:601–629, 1998.

[2] F. Ben Belgacem. The mortar finite element methodwith Lagrange multipliers. *Numer. Math.*, 84:173–197, 1999.

[3] F. Ben Belgacem, M. Fournié, N. Gmati, and F. Jelassi. On the Schwarz algorithms for the Elliptic Exterior Boundary Value Problems. *M2AN. Mathematical Modelling and Numerical Analysis*, 39(4):693–714, 2005.

[4] F. Ben Belgacem, N. Gmati, and F. Jelassi. Convergence bounds of GMRES with Schwarz preconditioner for the scattering problem. *Int. J. Numer. Meth. Engng.*, 80:191–209, 2009.

[5] A. Bendali, Y. Boubendir, and N. Zerbib. Localized adaptive radiation condition for coupling boundary with finite element methods applied to wave propagation problems. *IMA Numerical Analysis,(2014) 34 (3): 1240-1265.*

[6] A. Bendali and M. Fares. *Boundary Integral Equations Methods in Acoustics.* Saxe-Coburg Publications, Kippen, Stirlingshire, Scotland, 2008.

[7] Y. Boubendir, A. Bendali, and M. Fares. Coupling of a non-overlapping Domain Decomposition Method for a Nodal Finite Element Method with a Boundary Element Method. *International Journal for Numerical Methods in Engineering*, 73(11):1624–1650, 2008.

[8] D. Colton and R. Kress. *Integral Equation Methods in Scattering Theory.* John Wiley and Sons, New York, 1983.

[9] D. Colton and R. Kress. *Inverse Acoustic and Electromagnetic Scattering Theory*, volume 93 of *Series in Applied Mathematics.* Springer Verlag, New York, Berlin, Heidelberg, 1992.

[10] G. C. Hsiao and W. L. Wendland. *Boundary Iintegral Equations.* Springer, Berlin-Heidelberg, 2008.

[11] Jianming Jin. *The Finite Element Method in Electromagnetics, Second Edition.* John Wiley & Sons, New York, 2002.

[12] Y. Li and Z. Cendes. High-accuracy absorbing boundary conditions. *IEEE Ttransactions on Magnetics*, 31:1524–1529, 1995.

[13] William McLean. *Strongly Elliptic Systems and Boundary Integral Equations.* Cambridge University Press, Cambridge, UK, and New York, USA, 2000.

[14] J.-C. Nédélec. *Acoustic and Electromagnetic Equations: Integral Representations for Harmonic Problems.* Springer, Berlin, 2001.

[15] Youcef Saad. *Iterative Methods for Sparse Linear Systems.* PWS Pblishing Company, Boston, 1996.